Carbohydrate Polymers 94 (2013) 229–234

Contents lists available at SciVerse ScienceDirect

Carbohydrate Polymers

journal homepage: www.elsevier.com/locate/carbpol

Green synthesis of polysaccharide/gold nanoparticle nanocomposite: An efficient ammonia sensor

Sadanand Pandey*, Gopal K. Goswami, Karuna K. Nanda

Materials Research Centre, Indian Institute of Science, Bangalore 560012, India

ARTICLE INFO

Article history:
Received 18 July 2012
Received in revised form
15 November 2012
Accepted 7 January 2013
Available online 16 January 2013

Keywords:
Guar gum
Gold nanoparticles
Green synthesis

ABSTRACT

A low cost eco-friendly method for the synthesis of gold nanoparticles (AuNPs) using guar gum (GG) as a reducing agent is reported. The nanoparticles obtained are characterized by UV–vis spectroscopy, scanning electron microscopy (SEM), transmission electron microscopy (TEM) and X-ray diffraction (XRD). Based on these results, a potential mechanism for this method of AuNPs synthesis is discussed. GG/AuNPs nanocomposite (GG/AuNPs NC) was exploited for optical sensor for detection of aqueous ammonia based on surface plasmon resonance (SPR). It was found to have good reproducibility, response times of ~10 s and excellent sensitivity with a detection limit of 1 ppb (parts-per-billion). This system allows the rapid production of an ultra-low-cost GG/AuNPs NC-based aqueous ammonia sensor.

1. Introduction

Nowadays, demands for robust ammonia sensing systems are increasing (Timmer, Olthuis, & Van Der Berg, 2005). Particularly, detection systems for continuous monitoring (Masserini & Fanning, 2000) are needed because ammonia is toxic to many aquatic organisms even in very low concentrations. One of the industrial gases of interest is ammonia in the form of ammonium hydroxide because of its toxic and polluting nature. Large quantities of ammonia are released in the farming industries and also produced in the chemical industry for fertilizers or in refrigeration systems. Leakage of ammonia can lead to life-threatening situations. The safe allowed limit in which people can work is 20 ppm (parts-per-million). High concentrations (500 ppm or more) of ammonia can lead to severe burns on skin, eyes, throat, or lungs causing permanent blindness and lung disease (De la Hoz, Schueter, & Rom, 1996). There is considerable interest in measuring the amount of ammonia in the human body, as it can be an indicator of disorder or diseases like kidney and liver malfunction, asthma, diabetes, cancer, and ulcers (Ament et al., 1999; Narasimhan, Goodman, & Patel, 2001).

Ammonia sensors based on ZnO, In_2O_3 and SnO_2 nanostructures have been demonstrated (Rout, Hegde, Govindraj, & Rao, 2007). Films from conjugated polymers such as polyaniline have also been used to detect ammonia by changes of their conduction properties (Koul, Chandra, & Dhawan, 2001). The major drawbacks associated with these sensors are their operation at high temperatures and sophisticated instrumentation along with the detection limit. Room temperature ammonia sensors remain an area of continuous interest. It has been shown that β-Fe_2O_3 NPs can be used for the detection of aqueous ammonia at room temperature (Rahman, Jamal, Khan, & Faisal, 2011). Silver nanoparticles (AgNPs) as ammonia sensor in 1–50 ppm have been reported (Pandey, Goswami, & Nanda, 2012). It has been seen that the detection of ammonia can be based on position and amplitude of the surface plasmon resonance (SPR) band change with ammonia concentration.

Green synthesis of AuNPs by using hydroxyl propyl cellulose, fungal proteins of *Coriolus versicolor* and by leaf extract of *Dalbergia sissoo* has already been reported (Abdel-Halim & Al-Deyab, 2011; Sanghi & Verma, 2010; Singh, Baboota, Naik, & Singh, 2012). But the synthesis of AuNPs by using guar gum (GG) has not yet been reported so far. GG is a naturally occurring plant polysaccharide produce in abundance. India generates about 80% of the world's total GG production. It is easily available, non-toxic, eco-friendly, biodegradable and cost effective. GG is also a renewable and abundantly available industrial polysaccharide material having backbone of β-D-(1→4) mannopyranosyl units with α-D-galactopyranosyl units as side chains. Many modified GG-silica nanocomposites are known to act as efficient heavy metals adsorbents or as efficient flocculants (Singh, Pandey, Singh, & Sanghi, 2009; Tiwari, 2010, 2011; Tiwari, Mishra, Kobayashi, & Turner, 2012).

We have for the first time reported the green synthesis of AuNPs using aqueous solution of polysaccharide *Cyamopsis tetragonaloba* commonly known as GG from plants as reducing agent. Here the main efforts are focused on synthesis, characterization and application in detecting the aqueous ammonia concentration in liquid

* Corresponding author. Tel.: +91 80 22932996; fax: +91 80 23607316.
E-mail address: Sadanand.au@gmail.com (S. Pandey).

0144-8617/$ – see front matter © 2013 Elsevier Ltd. All rights reserved.
http://dx.doi.org/10.1016/j.carbpol.2013.01.009

phase by monitoring the absorbance spectra. Sensitivity, stability and reproducibility studies reveal excellent properties that can be explored as ammonia sensor for practical applications at room temperature. Our main focus has been ammonia detection at sub-ppm level.

2. Experimental

2.1. Materials

Gold (III) chloride hydrate ($HAuCl_4{\cdot}3H_2O$, 99.9%) purchased from Aldrich (USA) and used without further purification. GG and sodium hydroxide was purchased from Merck, Germany. All aqueous solutions were made using ultrahigh de-ionized (DI) water purified using a Mill-Q Plus system (Millipore Co.).

2.2. Preparation of GG/AuNPs NC using GG

All glassware used was cleaned in a bath of freshly prepared aqua regia solution (HCl:HNO_3, 3:1), and rinsed thoroughly with H_2O prior to use. For the synthesis of AuNPs, a stock solution of 10 mM was prepared by adding gold (III) chloride hydrate in DI water. Then, the gold (III) chloride hydrate solution was mixed with GG solution followed by the addition of few drop of very dilute solution of sodium hydroxide (0.01 M) at room temperature. Then, the solutions were stirred gently at the desired temperatures (80 °C) for 160 min to yield AuNPs. Here the yellow color solution was converted to the characteristics pink-red color solution indicating the formation of GG/AuNPs NC. It was observed that the aqueous solution of AuNPs was stable for more than eight months at room temperature.

2.3. Characterization of synthesized GG/AuNPs NC

The nanostructured materials are characterized by X-ray diffraction (XRD) using Bruker D8 Advance powder diffractometer operating in the reflection mode with CuKα radiation. The size of the NPs were determined with transmission electron microscope (TEM) using a TECHNAI T20 microscope operating at 200 kV equipped with an EDS (energy dispersive spectrum) detector. UV–vis spectroscopy was used to ensure the formation of NPs.

3. Results and discussion

3.1. UV–vis and TEM analysis of GG/AuNPs NC

It is well known that the optical properties of AuNPs depend strongly on the size, shape, interactions between the nanoparticles and their adsorbed species on the surface of the nanoparticles. Fig. 1A shows the UV–vis spectra of the GG/AuNPs NC formed at different molar concentrations of $HAuCl_4{\cdot}3H_2O$. In this experiment, AuNPs synthesized under conditions of lower concentration of $HAuCl_4{\cdot}3H_2O$ (1 mM), GG (2.5%, w/v) gave a brown suspension (a), whereas at higher molar concentration of gold salt (10 mM) the suspension was purple red (b). The color of the gold colloid arises because of the SPR absorption of AuNPs (Mulvaney, 1996). The sample solutions of AuNPs prepared here show an intensive SPR band around 539 nm. In general, the AuNPs often show an intense SPR band from 500 to 600 nm at the UV–vis (Szunerits & Boukherroub, 2006). According to the reported literature, the position of SPR absorption of AuNPs depends on their size and shape as well as their surrounding medium (Prasad, Stoeva, Sorensen, & Klabunde, 2003; Rechberger et al., 2003).

The formation of AuNPs was evidenced with the change in color of the solution after addition of gold salt from the yellowish to pink red color solution. The formation of GG/AuNPs NC was monitored through UV–vis spectrophotometer at time intervals from 10 to 160 min (Fig. 1B). The intensity of the peak increases gradually with increase of time. The spectrum obtained at 160 min shows the absorption maximum as 539 nm.

The UV–vis absorption spectra of AuNPs prepared using GG in different concentrations (0.125–3.5%, w/v), at initial pH of 8 and temperature of 80 °C for 160 min was measured. It was found that there is a gradual increase in the absorption intensity, by increasing the GG concentration up to 3.5% (w/v). It is worthy of mention here that the least amount of GG in the reaction medium (1%, w/v) is enough for full reduction of the Au^{3+} to Au^0 nanoparticles.

Investigation of the morphologies of the as-prepared GG/AuNPs NC was performed using TEM (Fig. 2A). NPs with spherical shapes are observed in Fig. 2A. The EDS equipped with TEM instrument confirms the presence of Au in the sample (Fig. 2B). A high-resolution TEM (HRTEM) image (shown in Fig. 2C) with clear lattice fringes having a *d*-spacing of 0.23, 0.20 and 0.14 nm reveals that the fcc crystal lattice with (1 1 1), (2 0 0) and (2 2 0) planes (JCPDS 46-1045). Fig. 2D shows the selected area electron diffraction (SAED) pattern of AuNPs. The clear lattice fringes in high resolution TEM image and the typical SAED pattern with bright circular rings correspond to the (1 1 1), (2 0 0), (2 2 0) and (3 1 1) planes. Fig. 2E shows the particle size distribution histograms of AuNPs formed after 160 min. The average particle size is found to be ~6.5 nm.

3.2. XRD studies

The XRD spectrum, for the synthesized GG/AuNPs NC is presented in Fig. 2F. It shows intensive characteristic peaks of metallic Au. Four main characteristic peaks for gold at 38.35, 44.36, 64.73 and 77.63 corresponding to Miller indices (1 1 1), (2 0 0), (2 2 0) and

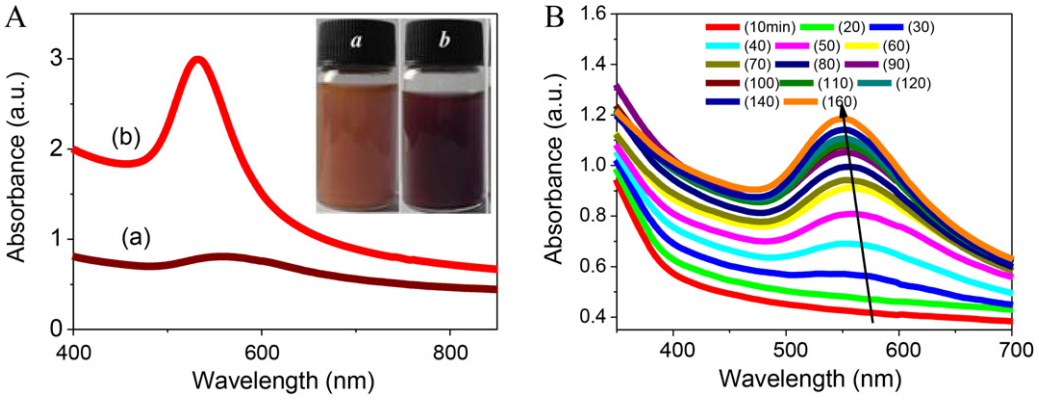

Fig. 1. (A) UV–vis spectra of AuNPs formed at different molar concentration (a) 1 mM; (b) 10 mM of $HAuCl_4$. (B) UV–vis spectra at different time interval.

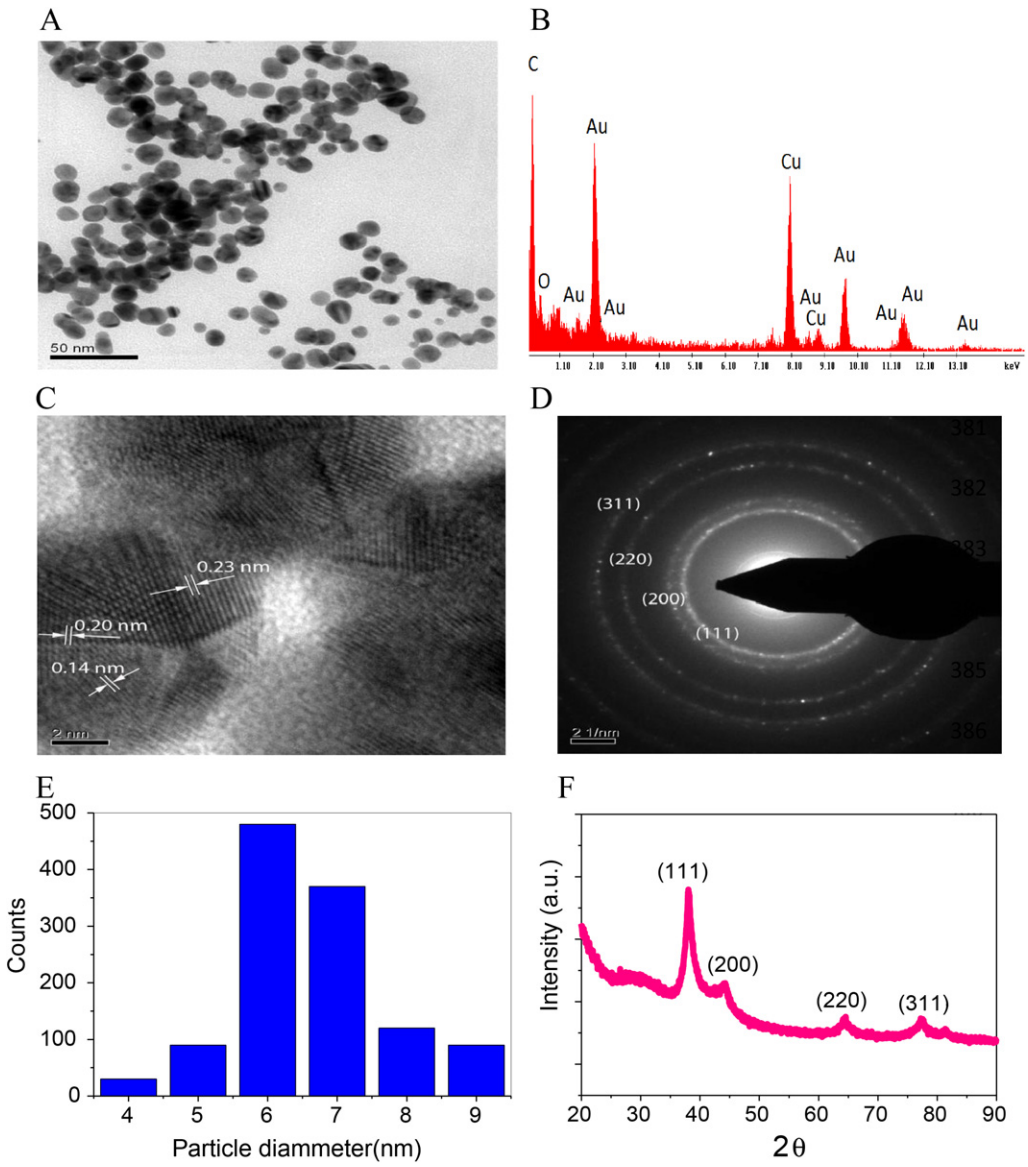

Fig. 2. (A) TEM of AuNPs. (B) HRTEM image with clear lattice fringe. (C) SAED pattern of AuNPs. (D) Particle size histogram of AuNPs. (E) EDS of AuNPs. (F) XRD pattern of AuNPs.

(311) were observed which confirmed the fcc crystalline geometry of AuNPs (JCPDS file no. 4-0784) based on the above XRD data.

3.3. *Ammonia sensing of GG/AuNPs NC*

The sensing study of ammonia solution was performed by optical measurements. To understand the optical properties of AuNPs, it is important to consider not only their composition, shape, and size but also the local environment (Kreibig & Vollmer, 1995). The local dielectric environment includes both solvent molecules as well as other NPs. When the electromagnetic fields from two different NPs interact, a complex SPR is produced (Ghosh & Pal, 2007). An important implication of NPs aggregation is shifting of the SPR to lower energies *versus* isolated NPs. In order to prevent uncontrolled aggregation, NPs surfaces have been modified with capping molecules that form an electrostatically induced steric barrier between NPs (Hunter, 1993). Alternatively, to allow controlled nanoparticle aggregation in specific environmental conditions, capping molecules can be assembled onto the surface of the NPs. Here GG is acting as a capping agent for stabilization of NPs. The hydroxyl groups in GG reduce the gold ions. A plausible mechanism for the formation of AuNPs has been shown in Fig. 3A. It appears that the AuNPs are encapsulated by the GG polymeric networks or Au–GG core–shell structure. The formed GG polymer networks facilitate the excellent stability of the NPs through electrostatic and steric effects and the hydroxyl groups of the polymeric chains, which further promote the stabilization of AuNPs. Because of the complexation ability of the polymer with AuNPs through the hydroxyl groups of the polymeric chains and networks, they surround and protect the particles over longer periods (Fig. 3A). On the other hand, a strong physical adsorption of the GG polymer onto the surface of the AuNPs is also an indication of better stabilization.

The stability of GG/AuNPs NC colloidal solution has been studied. No change in colors and visual aggregation has been observed even after eight months of storage. Besides, the absorbance spectrum of silver nanoparticles showed hardly any change in the position of SPR peak and intensity values. Hence, AuNPs formed by this method is highly stable and well dispersed in nature (Fig. 3B). The sensing property of NPs solution against increasing ammonia concentration in the range of 1–100 ppm by monitoring the changes in SPR position and amplitude with a UV–Visible spectrophotometer has been reported (Dubas & Pimpan, 2008; Pandey et al., 2012). In order

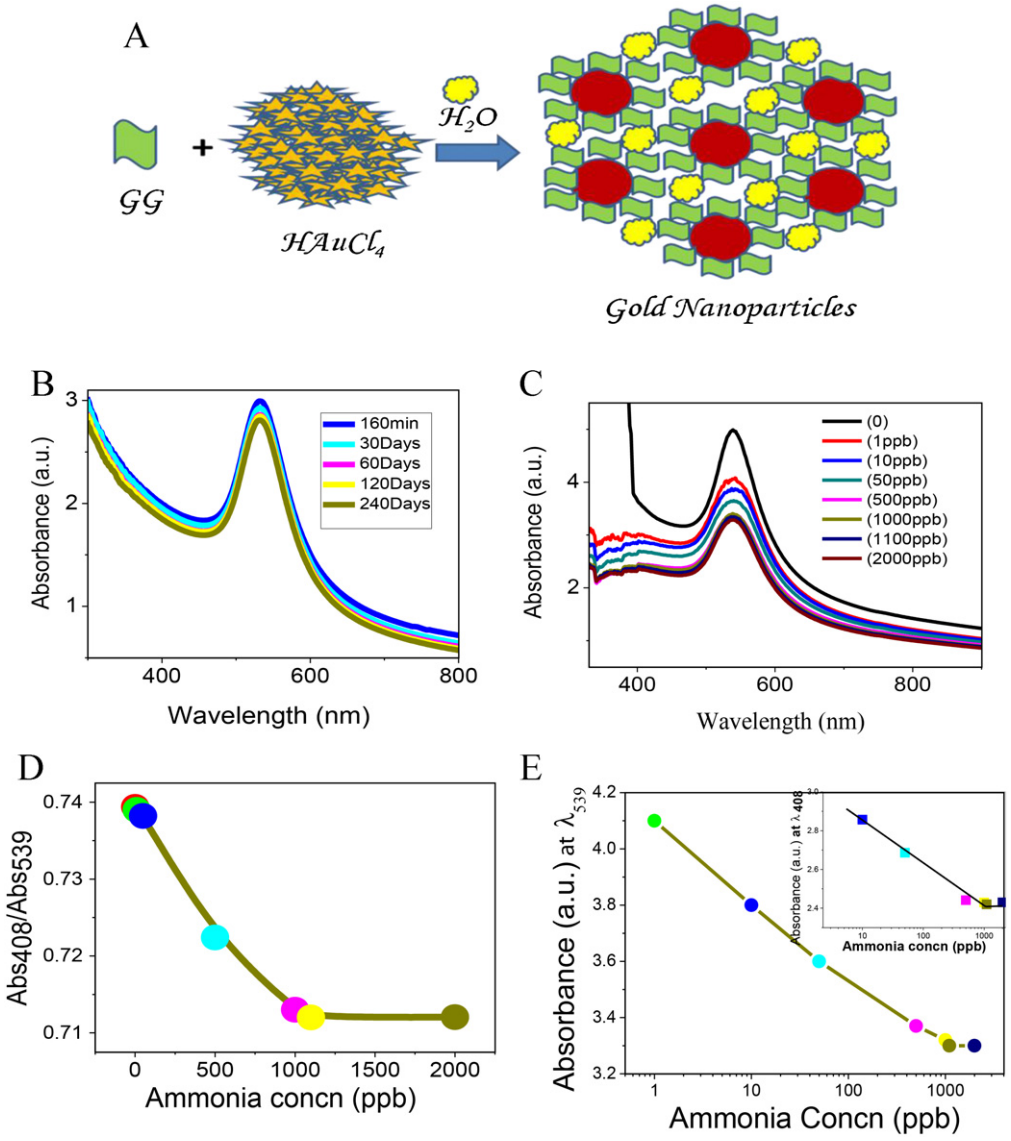

Fig. 3. (A) Mechanism for stabilization of NPs. (B) Stability of AuNPs. (C) Plot of change in spectral absorbance as a function of ammonia concentration. (D) Ratio of absorbance of wavelength ($\lambda_{408}/\lambda_{539}$) as a function of ammonia concentration. (E) Variation in absorbance at λ_{539} and λ_{408} (inset) as a function of ammonia concentration.

to study the ammonia sensing behavior, the GG/AuNPs NC solution was mixed with an aqueous ammonia solution at different concentrations of 1–2000 ppb by diluting with 25% ammonia solution in DI water immediately before the experiment. The initial ammonia concentration of 25% ammonia solution is calculated to be 227,500 ppm. From the original ammonia solution of 227,500 ppm, the desired ammonia concentration in the range of 1–2000 ppb can be easily prepared by dilution method.

The absorbance spectra of GG/AuNPs NC colloidal solution with different ammonia concentrations (0–2000 ppb) are shown in Fig. 3C. No blue shift is observed in the spectral absorbance. However, the absorbance peak intensity around 539 nm continuously decreases with increasing concentration of ammonia. A new peak at 408 nm appears when ammonia is added to the colloidal solution. Because of association of ammonia with Au^{3+} or Au^{+} ions lead to the formation of $[Au(NH_3)_2]^{3+}$ and $[Au(NH_3)_2]^{+}$ coordination complexes. Similar coordination complex formations with Ag NPs are reported earlier (Dubas & Pimpan, 2008). It has been shown for Ag NPs that the SPR shifts with ammonia concentration (Dubas & Pimpan, 2008; Pandey et al., 2012; Peng, McMahon, Schatz, Gray, & Sun, 2010). The blue shift in the SPR peak can be understood in terms of Mie theory (Shen & Liou, 2008). According to this theory, when an adsorbate donates electron to the NPs the SPR peak blue shifts which is given by

$$\lambda_m^2 = \frac{(2\pi c)^2 m}{4\pi n_e e^2}(\varepsilon_0 + 2n_0^2)$$

where ε_0 is the high frequency dielectric constant of the metal and n_0 is the refractive index. This equation indicates that the SPR wavelength is proportional to the inverse square root of the electron density. But in our case, no shift in the SPR peak position is observed for Au NPs colloidal solution by the addition of ammonia which is believed to be due to the local environment.

It is recognized that the optical property of metallic nanomaterials from SPR is caused by the collective oscillation of surface conduction electrons by light (Hutter & Fendler, 2004), thus the changes in the peak intensity of GG/AuNPs NC colloidal solution after the addition of different ammonia concentration (0–2000 ppb) are shown in Fig. 3C, which can also be explained based on variations in refractive index as the result of the binding of ammonia molecules to the GG/AuNPs NC. The results are in agreement with

Table 1
A comparative table of few reported ammonia sensors with GG/AuNPs NC.

Working medium	Lower detection limit	Response time	Temperature range (°C)	References
Au (0.8 wt.%)–MoO_3 (5 wt.%)–WO_3	1–50 ppm	–	400–500	Xu, Miura, Ishida, Matsuda, and Yamazoe (2000)
Pt/AlGaN/GaN Schottky-type ammonia gas sensor	35 ppm	–	150	Chen, Chen, Liu, Huang, and Hsu (2011)
Metal oxide (WO_3)	1 ppm	5 min	400	Xu et al. (2000)
WO_3 loaded with 1 wt.% metal oxides	30 ppm		350	Wang, Miura, & Yamazoe (2000)
ZnO nanorod	1–800 ppm	26 s	300	Rout et al. (2007)
Catalytic metal (palladium)	1 ppm	1 min	600	Winquist, Spetz, & Lundström (1984)
GG/Ag NPs NC	1 ppm	~s	RT	Pandey et al. (2012)
PMA/Ag NPs	5 ppm	–	RT	Dubas and Pimpan (2008)
GG/Au NPs NC	1 ppb	~10 s	RT	Present study

the earlier reports (Bendikov, Rabinkov, Karakouz, Vaskevich, & Rubinstein, 2008; Haes & Van Duyne, 2002; Hiep, Yoshikawa, Saito, & Tamiya, 2009; Hong, Lee, & Yi, 2011; Karakouz, Vaskevich, & Rubinstein, 2008). Thus we can conclude that the absorption peak and intensity can change drastically if the dielectric constant and refractive index of the medium is changed.

We have shown that the variation in the intensity of absorbance spectra can be used for the ammonia detection. The absorbance ratio as a function of ammonia concentration at two different wavelengths (abs_{408}/abs_{539}) as shown in Fig. 3D reveals a linear relationship with a correlation factor R^2 equal to 0.991 for the range of 1–1000 ppb. It is also clear that beyond 1000 ppb ammonia concentration, the ratio of the values (abs_{408}/abs_{539}) remains constant. We have also plotted the absorbance at individual wavelengths as a function of ammonia concentration (Fig. 3E and the inset). It is seen from Fig. 3E that the absorbance at both 539 and 408 nm varies logarithmically with ammonia concentration below 1000 ppb. Over all, the colorimetric method described here cannot be used beyond 1000 ppb.

We believe this is one of the simplest methods to detect the ammonia concentration in an aqueous solution by measuring the individual absorbance as well as the ratio of absorbance at two different wavelengths. Though the results are highly reproducible, the process is not reversible which indicates that GG/AuNPs NC colloidal solution can be used once for each ammonia concentration. However, the shelf-life of GG/AuNPs NC colloidal solution is more than eight months as discussed earlier. This indicates that the Au NPs prepared once can be used at least for eight months. Response time is measured based on the kinetic of color shift. It was found that the change in color was extremely fast and requires ~10 s. Thus the present studies on GG/AuNPs NC demonstrate the fast response and high sensitivity of the sensor.

A few reported ammonia sensors are summarized in Table 1. It can be noted that some of them are based on resistance measurements which work at high temperature. The sensors based on optical studies have also been reported mainly with AgNPs that can be used for detection at ppm level. But in the present study we have reported the use of cheap and easily available polysaccharide for AuNPs, which reduces the cost of sensor to many fold and secondly since it works at room temperature, so we do not need any external power supply for enhancing the sensor temperature. Furthermore, AuNPs can be used for the detection of ammonia at ppb levels.

Usually the presence of different compounds interferes with the sensitivity of the sensor. Interfering studies with different compounds for the amperometric detection of NO_2 gas are reported earlier (Tiwari & Gong, 2008a, 2008b). In order to understand the effect of interfering substances ethanol and methanol was added during ammonia sensing through optical measurement into GG/AuNPs NC ammonia solution. No change in the shift of SPR peak is observed. This clearly confirms that these two compounds are not interfering in the sensing of ammonia.

4. Conclusion

The present study reports the green synthesis of AuNPs. GG act as a reducing and capping agent. The stability study of AuNPs due to GG is found to be excellent. This is a low cost and eco-friendly method to synthesize the GG/AuNPs NC. Colorimetric assays based on the unique SPR properties of AuNPs have showed to be very useful due to their simplicity, high sensitivity, low detection limit of 1 ppb, low cost, fast response time and great reproducibility. It may be noted that we have reported room temperature detection of aqueous ammonia at ppb level by AuNPs based optical sensor. Keeping these significant properties in mind, in the near future we can use our room temperature optical ammonia sensor for clinical and medical diagnosis for detecting ultra low ammonia level in human.

Acknowledgement

One of the authors (SP) is thankful to Dr. D.S. Kothari postdoctoral fellowship of University Grant Commission (UGC), for its generous financial support. The authors also acknowledge financial assistance of Robert Bosch Center for Cyber Physical Systems for Lab facilities.

References

Abdel-Halim, E. S., & Al-Deyab, S. S. (2011). Utilization of hydroxypropyl cellulose for green and efficient synthesis of silver nanoparticles. *Carbohydrate Polymers*, *86*, 1615–1622.
Ament, W., Huizenga, J. R., Kort, E., Van Der Mark, T. W., Grevink, R. G., & Verkerke, G. J. (1999). Respiratory ammonia output and blood ammonia concentration during incremental exercise. *International Journal of Sports Medicine*, *20*, 71–77.
Bendikov, T. A., Rabinkov, A., Karakouz, T., Vaskevich, A., & Rubinstein, I. (2008). Biological sensing and interface design in gold island film based localized plasmon transducers. *Analytical Chemistry*, *80*, 7487–7498.
Chen, T.-Y., Chen, H.-I., Liu, Y.-J., Huang, C.-C., & Hsu, C.-S. (2011). Ammonia sensing properties of a Pt/AlGaN/GaN Schottky diode. *IEEE Transactions of Electron Devices*, *58*(5), 1541–1547.
De la Hoz, R. E., Schueter, D. P., & Rom, W. N. (1996). Chronic lung disease secondary to ammonia inhalation injury: A report on three cases. *American Journal of Industrial Medicine*, *29*(2), 209–214.
Dubas, S. T., & Pimpan, V. (2008). Green synthesis of silver nanoparticles for ammonia sensing. *Talanta*, *76*(1), 29–33.
Ghosh, S., & Pal, T. (2007). Interparticle coupling effect on the surface plasmon resonance of gold nanoparticles: From theory to applications. *Chemical Reviews*, *107*, 4797–4862.
Haes, A. J., & Van Duyne, R. P. (2002). A nanoscale optical biosensor: Sensitivity and selectivity of an approach based on the localized surface plasmon resonance spectroscopy of triangular silver nanoparticles. *Journal of the American Chemical Society*, *124*, 10596–10604.

Hiep, H. M., Yoshikawa, H., Saito, M., & Tamiya, E. (2009). An interference localized surface plasmon resonance biosensor based on the photonic structure of Au nanoparticles and SiO_2/Si multilayers. *ACS Nano*, *3*, 446–452.

Hong, S., Lee, S., & Yi, J. (2011). Sensitive and molecular size-selective detection of proteins using a chip-based and heteroliganded gold nanoisland by localized surface plasmon resonance spectroscopy. *Nanoscale Research Letters*, *6*, 336.

Hunter, R. J. (1993). *Introduction to modern colloid science*. New York: Oxford University Press., p. 344.

Hutter, E., & Fendler, J. H. (2004). Exploitation of localized surface plasmon resonance. *Advanced Materials*, *16*, 1685–1706.

Karakouz, T., Vaskevich, A., & Rubinstein, I. (2008). Polymer-coated gold island films as localized plasmon transducers for gas sensing. *Journal of Physical Chemistry B*, *112*, 14530–14538.

Koul, S., Chandra, R., & Dhawan, S. K. (2001). Conducting polyaniline composite: A reusable sensor material for aqueous ammonia. *Sensors and Actuators B*, *75*, 151–159.

Kreibig, U., & Vollmer, M. (1995). *Cluster materials*. Heidelberg, Germany: Springer-Verlag., p. 532.

Masserini, R. T., & Fanning, K. A. (2000). A sensor package for the simultaneous determination of nanomolar concentrations of nitrite, nitrate, and ammonia in seawater by fluorescence detection. *Marine Chemistry*, *68*, 323–333.

Mulvaney, P. (1996). Surface plasmon spectroscopy of nanosized metal particles. *Langmuir*, *12*, 788–800.

Narasimhan, L. R., Goodman, W., & Patel, N. (2001). Correlation of breath ammonia with blood urea nitrogen and creatinine during hemodialysis. *Proceedings of the National Academy of Sciences of the United States of America*, *98*, 4617–4621.

Pandey, S., Goswami, G. K., & Nanda, K. K. (2012). Green synthesis of biopolymer-silver nanoparticle nanocomposite: an optical sensor for ammonia detection. *International Journal of Biological Macromolecules*, *51*, 583–589.

Peng, S., McMahon, J. M., Schatz, G. C., Gray, S. K., & Sun, Y. (2010). Reversing the size-dependence of surface plasmon resonances. *Proceedings of the National Academy of Sciences of the United States of America*, *107*, 14530–14534.

Prasad, B. L. V., Stoeva, S. I., Sorensen, C. M., & Klabunde, K. J. (2003). Digestive-ripening agents for gold nanoparticles: alternatives to thiols. *Chemistry of Materials*, *15*, 935–942.

Rahman, M. M., Jamal, A., Khan, S. B., & Faisal, M. (2011). Characterization and applications of as-grown β-Fe_2O_3 nanoparticles prepared by hydrothermal method. *Journal of Nanoparticle Research*, *13*, 3789–3799.

Rechberger, W., Hohenau, A., Leitner, A., Krenn, J. R., Lamprecht, B., & Aussenegg, F. R. (2003). Optical properties of two interacting gold nanoparticles. *Optics Communications*, *220*, 137–141.

Rout, C. S., Hegde, M., Govindraj, A., & Rao, C. N. R. (2007). Ammonia sensors based on metal oxide nanostructures. *Nanotechnology*, *18*, 205504.

Sanghi, R., & Verma, P. (2010). pH dependant fungal proteins in the 'green' synthesis of gold nanoparticles. *Advanced Materials Letters*, *1*(3), 193–199.

Shen, C. Y., & Liou, S. Y. (2008). Surface acoustic wave gas monitor for ppm ammonia detection. *Sensors and Actuators B*, *131*, 673–679.

Singh, C., Baboota, R. K., Naik, P. K., & Singh, H. (2012). Biocompatible synthesis of silver and gold nanoparticles using leaf extract of *Dalbergia sissoo*. *Advanced Materials Letters*, *3*(4), 279–285.

Singh, V., Pandey, S., Singh, S. K., & Sanghi, R. (2009). Removal of cadmium from aqueous solutions by adsorption using poly(acrylamide) modified GG–silica nanocomposites. *Separation and Purification Technology*, *67*, 251–261.

Szunerits, S., & Boukherroub, R. (2006). Electrochemical investigation of gold/silica thin film interfaces for electrochemical surface plasmon resonance studies. *Electrochemistry Communications*, *8*, 439–444.

Timmer, B., Olthuis, W., & Van Der Berg, A. (2005). Ammonia sensors and their applications—A review. *Sensors and Actuators B*, *107*, 666–677.

Tiwari, A. (2010). *Polysaccharides: Development, properties and applications*. New York, USA: Nova Science Publishers, Inc., ISBN 978-1-60876-544-7.

Tiwari, A. (2011). *Recent developments in bio-nanocomposites for biomedical applications*. New York, USA: Nova Science Publishers, Inc., ISBN 978-1-61761-008-0.

Tiwari, A., & Gong, S. (2008a). Electrochemical synthesis of chitosan-*co*-polyaniline/$WO_3 \cdot nH_2O$ composite electrode for amperometric detection of NO_2 gas. *Electroanalysis*, *20*, 1775–1781.

Tiwari, A., & Gong, S. (2008b). Vacuum-deposited poly(o-phenylenediamine)/$WO_3 \cdot nH_2O$ nanocomposite thin film for NO_2 gas sensor. *Polymer Journal*, *41*, 726–732.

Tiwari, A., Mishra, A. K., Kobayashi, H., & Turner, A. P. F. (2012). *Intelligent nanomaterials*. Salem, USA: Wiley-Scrivener Publishing LLC., ISBN 978-04-709387-99.

Wang, X., Miura, N., & Yamazoe, N. (2000). Study of WO_3-based sensing materials for NH_3 and NO detection. *Sensors and Actuators B: Chemical*, *66*, 74–76.

Winquist, F., Spetz, A., & Lundström, I. (1984). Determination of ammonia in air and aqueous samples with a gas-sensitive semiconductor capacitor. *Analytica Chimica Acta*, *164*, 127–138.

Xu, C. N., Miura, N., Ishida, Y., Matsuda, K., & Yamazoe, N. (2000). Selective detection of NH_3 over NO in combustion exhaust by using Au and MoO_3 doubly promotedWO_3 element. *Sensors and Actuators B*, *65*, 163–165.